Cellulose (2024) 31:5097–5114
https://doi.org/10.1007/s10570-024-05886-w

ORIGINAL RESEARCH

A preliminary study on 3D printing feedstock derived from cellulose recovered from cigarette butts

Flavia D'Urso · Paolo Iaccarino · Michele Giordano · Maria Oliviero · Ernesto Di Maio · Lucia Sansone

Received: 22 January 2024 / Accepted: 29 March 2024 / Published online: 16 April 2024

Abstract In this work, we describe the recovery of cellulose acetate (r-CA) polymer from waste cigarette butts (CBs) and their subsequent conversion into feedstock for 3D printing technology. The extraction process for CBs includes two stages: initial washes in water, followed by additional washes in ethanol. A final step involves a dissolution and reprecipitation process, resulting in the creation of a fine powder. The recovery polymer has been analysed and compared to commercial cellulose acetate (p-CA) and unsmoked cigarette filter (u-CA) to assess its purity and examine alterations in its physicochemical properties. The CA powder has also been plasticized with different biocompatible plasticizers to improve the mechanical properties of the CA. We analyze the rheological properties to identify the suitable composition as feedstock for 3D printing.

Keywords Cigarette butts · Cellulose acetate · Extraction process · Recovery · 3D printing

Flavia D'Urso and Paolo Iaccarino contributed equally to this work.

F. D'Urso · M. Giordano · M. Oliviero · L. Sansone (✉)
Institute for Polymers, Composites and Biomaterials, National Research Council of Italy (CNR), 80055 Portici, Italy
e-mail: lucia.sansone@cnr.it

P. Iaccarino
Scuola Superiore Meridionale, Largo San Marcellino 10, 80138 Naples, Italy

P. Iaccarino · E. Di Maio
Dipartimento Di Ingegneria Chimica, Dei Materiali E Della Produzione Industriale, University of Naples Federico II, Piazzale Vincenzo Tecchio, 80, 80125 Naples, NA, Italy

Introduction

Cigarette butts (CBs) are one of the most common types of litter around the world. The main problem with this waste is its method of disposal by smokers. As most smokers do not properly dispose of CBs in trash cans and discard them anywhere, collecting this litter is a difficult and costly process. This has caused CBs to be observed extensively in various urban areas and public places with consequent effects on environmental resources and living organisms (Jungst et al. 2016; Kalsoom et al. 2016; Kirchmajer et al. 2015; Ligon et al. 2017a, b; Wang et al. 2017; Auriemma et al.2022; Araújo and Costa 2019; Torkashvand et al. 2020). The CBs are, in fact, known as toxic litters. In CBs, there are many pollutants derived from fertilizers used in tobacco cultivation, from processing and cigarette assembly, and formed during smoking. Heavy metals such as lead, cadmium, copper, nickel, zinc and chromium are recognized contaminants found in CBs, seeping into the environment, and potentially entering the food chain (Valiente et al. 2020; Kataržytė et. 2020; Yousef et al. 2021a, b; Yousef et al. 2021a, b; Torkashvand et al.

2021; Torkashvand et al. 2022; Dobaradaran et al. 2017; Ghasemi et al. 2022). Alongside heavy metals, CBs contain various identified pollutants, including organic compounds, PAHs, and nicotine (Yousef et al. 2021a, b). Multiple studies indicate that these pollutants escape from discarded CBs, disperse, and contaminate the environment. The extent of this pollutant release depends on its initial concentration in the CB and environmental factors such as humidity (Dobaradaran et al. 2020). This leakage from CBs leads to water and soil contamination, and the demonstrated toxicity of CBs on many organisms underlines the severity of the issue in several cases. The possibility of ingestion of CBs by pet, infants and fish is another consequence of CBs littering (Dobaradaran et al. 2020; Green et al. 2019; Kurmus and Mohajerani 2020; Dieng et al. 2013; Dieng et al. 2014; Lee and Lee 2015; Slaughter et al. 2019; Parker and Rayburn 2017; Novotny et al. 2011). The CBs are constituted by the listed toxic chemicals from the microfibers of cellulose acetate (CA) (Belzagui et al. 2021; Conradi and Sanchez-Moyano 2022) and so they are also responsible for micro-plastic pollution in the aquatic environment. Extracting value-added materials, such as CA, from such waste for the manufacturing of new products could allow a reduction in both the overall ecological footprint and the cost of waste mitigation.

As mentioned already, nowadays there is no sustainable disposal method for these wastes. A recycling technology for cigarettes butts has not yet been established. Hence, repurposing cigarette butts could aid in the conservation of natural resources and offer an eco-friendly disposal solution. Presently, researchers are exploring avenues to create sustainable products from waste, such as composites (Mahmud et al. 2022) and eco-friendly materials (Islam et al. 2022). The recycling of cigarettes butts presents challenges due to the lack of straightforward methods for efficient separation or cost-effective treatment of chemicals trapped within filters. However, various researchers have investigated different applications of cigarette butts in recycled materials, including nonwoven production (De Vielmo et al. 2022), sound absorbing materials (Gómez Escobar et al. 2021), nanocrystal cellulose (Browne 1990), support materials for brick and steel manufacturing (Abdullatif et al. 2020), Asphalt Concrete (Rahman et al. 2020), energy storage in supercapacitor electrodes (Lee et al. 2014), and cellulose acetate fiber extraction with properties characterization (De Fenzo et al. 2020). Furthermore, Mohajerani et al. (2016) explored the recycling of CB in fired clay bricks, while in (Mohajerani et al. 2017), they proposed their use as aggregates in asphalt mixtures, along with a method to recover cellulose acetate from cigarettes for incorporation into stone mastic asphalt (SMA) mixtures. The European Waste List (https://eur-lex.europa.eu/legal-content/.) does not categorize cigarette butts specifically but classifies them under "Municipal waste including separately collected fraction other fractions not otherwise specified." Therefore, it is crucial to adopt the precautionary principle and raise awareness among consumers and producers to reduce tobacco waste production and environmental impact. Current disposal methods such as landfilling or incineration are unsustainable and costly. Thus, developing a recycling method for tobacco waste would mitigate environmental pollution and promote material recovery aligned with the principles of circular economy and sustainable development. Many studies on CB treatment focus solely on smoked CBs and lack comparative analysis with nonsmoked material. Typically, samples are physically separated and crushed into small fragments for treatment, with the resulting solid materials finding applications in various sectors such as construction, energy, environment, and chemistry. Authors often omit to describe CB sample collection methods because laboratory applications require minimal quantities. However, effective collection and handling are crucial to the effectiveness of the treatment process and economic viability. Inadequate collection and handling may compromise product efficacy and economic feasibility. The CB management treatment processes are primarily on a laboratory pilot scale, lacking large-scale analysis or experimental application that simulates operational processes with greater quantities and critical barriers. Although there have been some recent scientific contributions, the majority are recent, indicating the global urgency for effective CB management. Increased citizen awareness and proper disposal habits could improve CB sample collection at designated points, facilitating more effective waste management practices.

In recent times, three-dimensional (3D) printing has rapidly emerged as a promising technology for creating intricate structural designs. Among the various 3D printing methods, extrusion-based printing, also known as Direct Ink Writing (DIW), is notable

for its versatility in material usage, ease of operation, and cost-effectiveness. The most used materials in 3D printing are polymers, composites, metals, ceramics, sand, and wax (Jungst et al. 2016; Kalsoom et al. 2016; Kirchmajer et al. 2015; Ligon et al. 2017a, b; Wang et al. 2017). Volatile organic compounds and ultrafine aerosols that could be harmful to humans are detected in 3D printing processes. 3D printed objects with such polymers are measurably toxic to zebrafish embryos, a model organism widely used in biological research (Oskui et al. 2015). Designing and manufacturing low-emitting and less toxic 3D printing materials are imminent. To reduce related safety risks and unpleasant smells with synthetic polymers, manufacturers and end-use customers are inclined toward using natural polymers, which are renewable and biodegradable (Rejeski et al. 2018). Much attention has been paid to the development of printable biopolymer composites with improved performance. Natural polymer hydrogels such as collagen, alginate, chitosan, and hyaluronic acid have been used to prepare scaffolds by 3D printing and showed great potential in promising new fields of tissue engineering and regenerative medicine (Chimene et al. 2016; Jungst et al. 2016; Shen et al. 2016). 3D printing of cellulosic materials presents an opportunity to fabricate 3D objects from a cheap and sustainable source. 3D printed cellulose materials in combination with other polymers are being studied extensively for versatile applications (Gatenholm et al. 2016; Li et al. 2016; Ligon et al. 2017a, b; Piras et al. 2017; Sultan et al. 2017). Cellulose-based materials, without chemical alteration, are generally deemed impractical for extrusion-based 3D printing due to their thermal decomposition before achieving a meltable, flowable state upon heating (Bao et al. 2015). This is attributed to the robust hydrogen bonding among the cellulose molecules. Previous scientific literature on 3D printing using cellulose-derived materials has typically focused on incorporating these materials as low-density fillers within another matrix, commonly another polymer, or using them to produce aerogel-like structures. However, the obtained 3D objects show a low density and dimensional stability. For this reason, alternative strategies must be studied and developed for cellulose-derived materials, such as cellulose acetate.

In this paper, a new method is proposed to obtain a novel feedstock for 3D printing with cellulose-based materials by recovering CB waste in alternative to fossil-based plastic materials. The method is based on the combined use of appropriate solvents and plasticizers to address the rheological and printability issues associated with DIW. The function of solvents and plasticizers is to temporarily reduce the strength of hydrogen bonding between molecules of CA and to enable a 3D printing process. A green process that uses water and ethanol is proposed to extract CA fibers from CB waste paired with a dissolution–precipitation technique for recovered CA powder. The morphological analysis of recovered CA fibers and powder has been evaluated by using SEM. The presence of metals, in particular heavy metals, has also been investigated by means of atomic absorption analysis. To evaluate the quality of recovered CA obtained, the results of chemical (FTIR), thermal (TGA, DSC), and mechanical (DMA) properties of films based on recovered CA obtained by means of a solvent cast process have been compared to those obtained for films of CA extracted from commercial and unsmoked filters, and of commercial pure powder CA. Different plasticizers, such as Triacetin and Polyethyleneglycol 400 at fixed percentages (Liu et al. 2019; Quintana et al. 2013; De Fenzo et al. 2020) have also been used, as an alternative to the currently most widespread industrial plasticizers, such as Diethyl phthalate and Triphenylphosphate, to assess the influence of plasticizer types on the chemical, thermal and mechanical properties of films based on recovered CA. The results obtained have been utilized to produce solutions as inks with different solvents, such as ethanol, dimethyl sulfoxide, or a mixture of these and selected plasticizers. The rheological behavior of these solutions has been analyzed in various solvent contents to identify the most suitable solvent or mixture of solvents and content for the preparation of feedstock for 3D printing technology with CA recovered from CBs (Jungst et al.2016; Tekin and Çulfaz-Emecen 2023; Cafiero et al. 2023). A comparison with the rheological behavior of solutions based on pure powder CA has also been conducted.

Materials and Methods

Materials

Smoked CBs have been collected by Essequadro Eyewear Company S.r.l. (Italy). To evaluate the effect of smoking on the quality of recovered CA, unsmoked

cigarette CBs of the RIZLA® brand (uCA) have been purchased and used in this work. The CA powder was supplied from Merck Life Science (Milano, Italy) and used as a pure reference material (p-CA). Distilled water (DI), acetone 99% v/v, ethanol 99% v/v, dimethyl sulfoxide, triacetin (TAC) and polyethylene glycol 400 (PEG 400) were purchased from Merck Life Science (Milano, Italy). All reagents were used as received.

Green Extraction and Precipitation of CA

The CBs were sterilized in an autoclave for 1 h at a temperature of 120 °C and 1 bar and, then washed in cold water three times to extend the CA fibers and in ethanol 99% w/w twice to remove potential organic compounds (see De Fenzo et al. 2020). During sterilization and washing with water and ethanol, heavy metals have also been removed. The extraction of cellulose acetate from the cleaned CBs has been performed by using a dissolution-reprecipitation technique to obtain a cellulose acetate powder. In particular, the cleaned CBs were dissolved in acetone (5% w/w) for 1 h at room temperature and then centrifuged to remove any trapped residues in the filter, mainly soot. The solution was kept in the ice bath and a nonsolvent (ethanol or water) was added dropwise. The solvent/nonsolvent ratio is 1:2. The precipitate was recovered with filtration and washed twice with ethanol. Finally, the powder was dried at 80 °C for 1 h in the oven. The scheme of the recovery process of CA from CBs is reported in Fig. 1. The recovered cellulose acetate powder is hereafter denoted as r-CA. The same procedure has been used to extract cellulose acetate from unsmoked filters RIZLA®. In this case, the extracted cellulose acetate is hereafter denoted as u-CA.

In Fig. 1, we show the scheme procedure; the collected cigarette butts have been sterilized in a water autoclave at a temperature of 120° C, after the sterilized CA has been subjected to some washing in water and ethanol; the recovered CA has been characterized to evaluate possible dangerous substances as reported with major details in the paper by De Fenzo et al. 2020; finally, the dissolution and reprecipitation technique have been used to obtain the r-CA, u-CA, and p-CA powders. Since CA is a fibrous material, CA powder cannot be obtained by a mechanical process, so, when we grind the fibers, we obtained fibers with controlled dimensions on the micron scale.

Fig. 1 Scheme of the recovery process of CA from CBs

Preparation of CA Films

Films based on different CA (r-CA, u-CA, and p-CA) were produced by the solvent casting technique. CA was dried in the oven until a constant weight was observed. Then, 0.5 g of CA was dissolved in 12 mL of acetone followed by stirring (800 rpm) at room temperature for 1 h. The prepared solution was then filtered to remove dust and other traces of impurities. The solution was left at room temperature for two hours to remove air bubbles. The prepared clear solution was cast onto polystyrene Petri dishes for film formation and then stored in plastic bags until use. All films obtained were very transparent and free of air bubbles. The same procedure has been used to produce films based on plasticized r-CA with 15 wt% TAC and 10 wt% PEG 400, hereafter denoted as r-CA 15% TAC and r-CA 10% PEG. In this case, plasticizers were added to the solution after the dissolution of r-CA in acetone and the resulting solution was stirred for another 10 min to obtain a good dispersion of plasticizer. Film thickness was measured using a digital micrometer (Mitutoyo, Japan); it was approximately 500 µm.

Preparation of CA solutions

Solutions of different compositions have been prepared as follows to evaluate the possible use in 3D printing. In a 5 mL vial, 0.5 g of CA was weighed, and 4 mL of solvent or solvent/co-solvent was added dropwise while manually mixing. This solution was placed in an ultrasonic bath for 20 min until complete homogenization. The composition of the polymer solutions prepared for rheological studies is shown in Table 1.

Table 1 Composition of CA solutions for rheological studies

Sample	CA [% wt]	Acetone [% wt]	DMSO [% wt]
r-CA-15-AC	15	85	-
r-CA-20-AC	20	80	-
r-CA-25-AC	25	75	-
r-CA-20-AC-D	20	40	40
p-CA-20-AC-D	20	40	40
p-CA-20-D	20	-	80

Sample characterization

To evaluate both structural/morphological properties and thermodynamic/functional properties of CA samples, several experimental techniques have been used.

Scanning electron microscopy and X-ray microanalysis (SEM–EDX): The morphology of fibers and powders of r-CA has been investigated by using a scanning electron microscope (Quanta 200 FEG, FEI, The Netherlands). Before SEM analysis, the samples were coated with a thin layer (about 10 nm thick) of an Au–Pd alloy using a sputter coating system (Emitech K575, Quorum Technologies LTD, UK). X-ray microanalysis was performed with the EDX Inca Oxford 250 instrument. The cut directions were the same for all samples.

Atomic Absorption Spectrometry: the analysis of heavy metals present in r-CA has been performed by using an atomic absorption spectrometer (Perkin Elmer Analyst 700, Norwalk, CT, USA) with a deuterium background corrector. All measurements were performed in an air/acetylene flame. A 10 cm long slot-burner head, a lamp, and an air–acetylene flame have been used. r-CA was dissolved in 0.5 mL of concentrated HNO_3 and made up to 5 mL with distilled water for analysis.

Thermogravimetric analysis (TGA): the thermogravimetric analysis of films was performed by using a Q500 TGA (TA Instruments, New Castle, Delaware, USA). The samples were heated from 30 to 450 °C at a heating rate of 5 °C/min under nitrogen and from 450 to 600 °C under air.

Thermally modulated differential scanning calorimetry (TMDSC): the temperature modulated differential scanning calorimetry of the films was performed with a Q 2000 DSC (TA Instruments, New Castle, Delaware, USA) under nitrogen atmosphere (50 mL/min); analysis has been carried out with a heating rate of 5 °C/min, modulation amplitude ± 2 °C, and modulation period of 40 s.

Fourier-transform infrared spectroscopy (FT-IR): FT-IR analyses of films have been performed using a System 2000 FT-IR (Perkin–Elmer, Waltham, MA, USA) at ambient temperature. The samples were analyzed in ATR spectra mode from 4000 to 600 cm^{-1} with a wavenumber resolution of 4 cm^{-1} for 64 scans. These analyses were performed in the ATR mode to estimate the principal chemical bonds

present in the samples and to verify any changes induced by the processes.

Contact angle measurements: the hydrophilicity of the films has been characterized by water contact angle measurements using a contact angle meter (CA, OCA20, Data physics, Germany). A drop (3 µL) of distilled water has been deposited on at least ten different sites on the surface of the film and the contact angles have been determined at the right and left ends of the drop. The contact angle value was calculated by averaging the measured values.

Dynamic mechanical thermal analysis (DMTA): the thermo-mechanical properties of the films have been investigated in shear mode (2 gaps configuration, 5 mm each) using a DMA + 1000 Metravib (ACOEM, Limonest, France SAS). The films have been cut into rectangular samples with a length of 35 mm and width of 15 mm. Thickness was measured using an outside analog micrometer (0–25 mm model, INECO s.r.l., Osnago, Italy). The linear viscoelastic regime has been preliminary investigated in p-CA samples by performing a strain sweep test at room temperature (25 ± 2 °C) and with a frequency of 10 Hz. The upper limit has been found to be 0.08% of strain. DMTA measurements have been made at a frequency of 10 Hz with a dynamic strain of 0.03%. The temperature ramp has been set at 2 °C/min with a temperature ranging from 25 °C to 250 °C. Transition temperatures were determined from the peak of the damping factor (*tan δ*) plot, the error being within ± 2 °C. Each test has been repeated three times.

Rheological Measurements: rheological measurements were performed using a stress controlled rotational rheometer (RheoScope MARS II, HAAKE, Germany) equipped with 20 mm parallel plates. The tests were carried out at 25 °C under nitrogen atmosphere, with a gap thickness of 0.2 mm. A solvent trap was used to prevent solvent evaporation. Frequency sweep tests were performed from 0.1 to 100 Hz with a fixed strain of $\zeta = 0.1\%$ were carried out to operate in the linear viscoelastic region.

Results and Discussion

Morphological and Elemental Analysis

The morphological evolution of the reprecipitation processes from CA fibers to powder is depicted in Fig. 2. The r-CA fibers produced before the extraction process are shown in Fig. 2a). The morphological investigation of the r-CA shows that the fiber surface turned smoother after sterilization and washing treatments. Furthermore, it has been feasible to determine by EDX analysis that a titanium coating covers the fibers. There are additional heavy metals, including lead (Pb), cadmium (Cd), and zinc (Zn). Cigarette filters are white because of titanium (Ti), which is found as titanium oxide. Instead, as shown in Fig. 2b), the r-CA powder produced by the dissolution-reprecipitation step exhibits a collapse of the fiber structure and a decrease in the concentration of Ti and heavy metals. For the analysis of the composition of fiber and powder, three different areas of each sample were analyzed and the average values are shown in the tables in Figs. 2a) and 2b). These data have been confirmed by heavy metal research by atomic absorption spectrometry. The results have recorded the concentration of 0.02 ppm of Pb, 0.05 ppm of Zn, and 0.03 ppm of Cd and the presence of 0.04 ppm of Ti for the r-CA powder. For the unsmoked filter (u-CA) the results show a concentration of 0.08 ppm of Ti and 0.03 ppm of Pb. Micevska et al. (2006) suggest that the toxicity of cigarette filters is also related to the presence of heavy and trace metals. These metals, especially heavy metals such as lead (Pb) and cadmium (Cd), are found in various brands of cigarette filter because of factors such as tobacco cultivation, soil pollution, pesticide and herbicide use, cigarette production processes, and the inclusion of brightening agents in the paper such as titanium dioxide.

Thermal and FTIR Analysis

The thermal decomposition of r-CA and p-CA was divided into two weight loss stages, corresponding to the slow pyrolysis and fast pyrolysis stages, while u-CA presents three weight loss stages (see Fig. 3a)). For r-CA and p-CA there is the largest mass loss of the sample at ~ 89.29% and ~ 79.04% respectively, which represents the main decomposition stage. This stage is characterized by a DTG peak located at a temperature of 346 °C, which is attributed to the thermal decomposition (pyrolysis) of cellulose acetate (Yousef et al. 2022). In the second reaction stage, the sample mass loss is ~ 9.2%, with a residual mass of ~ 0.8% at 600 °C for r-CA, while the sample mass loss is ~ 15%, with a residual mass of ~ 0.6% at 600 °C

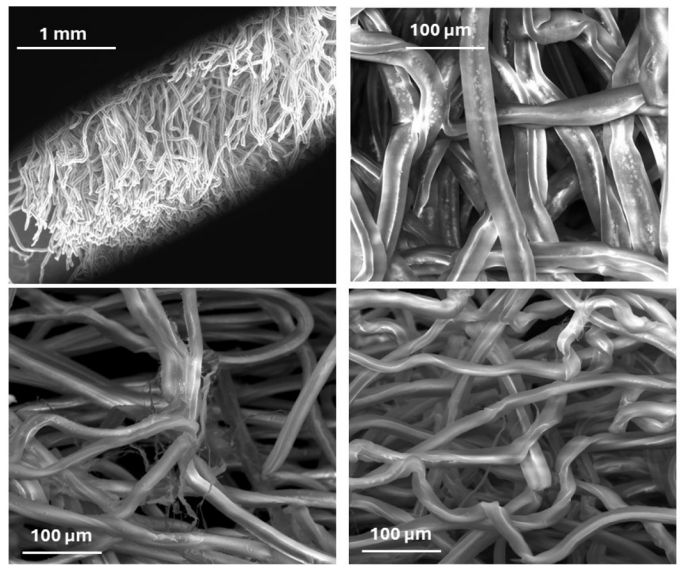

a)

	C	O	Ti	Zn	Cd	Pb
%w/w	48.4	57.5	2.37	0.36	0.35	0.41

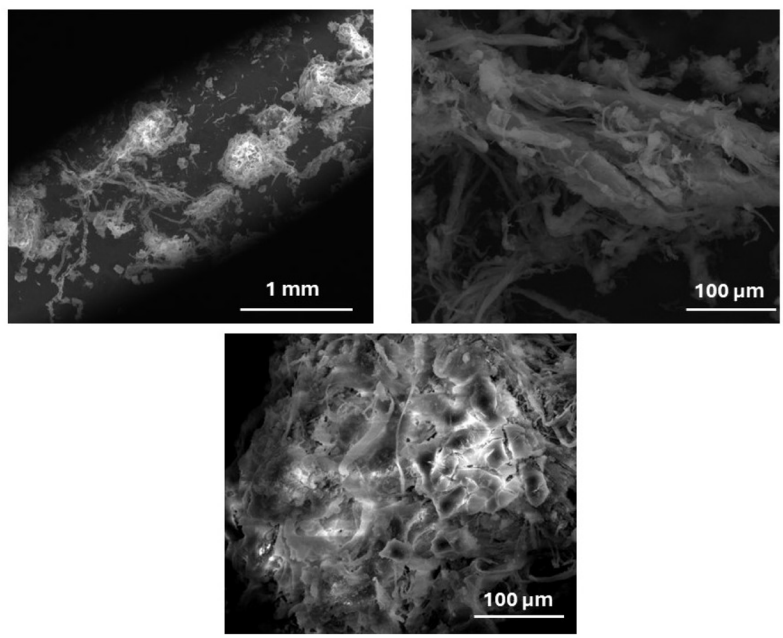

b)

	C	O	Ti	Zn	Cd	Pb
%w/w	48.0	56.5	1.37	0.22	0.05	0.27

Fig. 2 SEM images of a) r-CA fibers after green treatment and b) r-CA powder obtained by the dissolution-reprecipitation technique and chemical composition related to EDX microanalysis

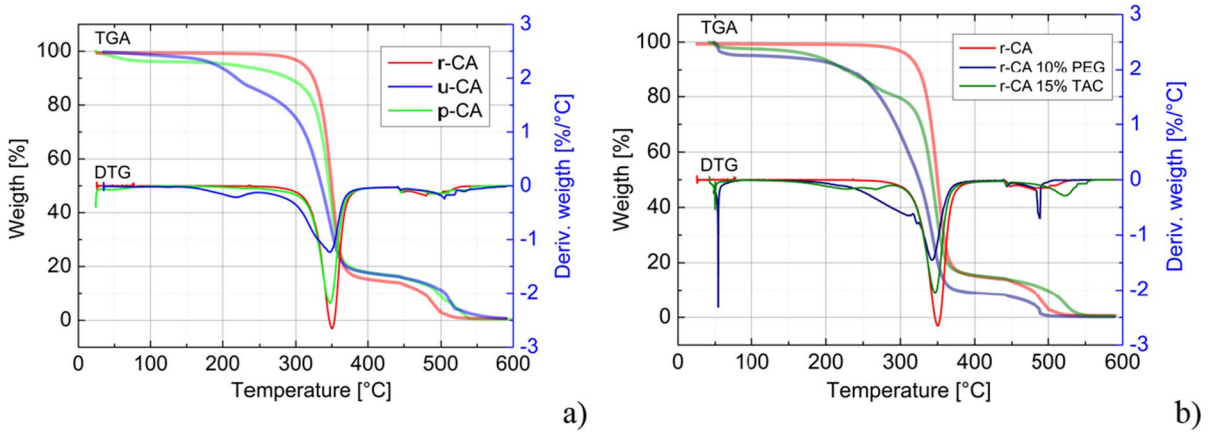

Fig. 3 **a** TGA and DTG curves of films r-CA, u-CA, and p-CA films; **b** TGA and DTG curves of films r-CA, r-CA 10% PEG and r-CA 15% TAC

for p-CA (Fig. 3a); u-CA presents a significant mass loss of ~ 8.5% manifesting as a DTG peak at 267 °C (Fig. 3a), and this reaction stage is attributed to the thermal decomposition of the plasticizer (Dreux et al. 2019). The cigarette filter that we have named u-CA comprises thin fibers of cellulose acetate aimed at improving filtration efficacy by intercepting a portion of the smoke to prevent inhalation. These fibers have a diameter of approximately 20 µm and undergo titanium dioxide (TiO_2) treatment to decrease their sheen. Subsequently, they are assembled into units containing 15000 fibers, using glycerol triacetate (triacetin (TAC)) as a binding agent to form the filter. TA serves as a common plasticizer for cellulose acetate filters, with typical values ranging between approximately 6% and 9% of the total filter weight, to achieve the desired hardness (Finster et al. 1986). Numerous scientific studies (Bonanomi et al. 2020), (Araújo and Costa 2019), (Bao et al. 2015), indicate that cellulose acetate differs from conventional cellulose due to its plasticized nature. In addition, various chemicals are used for paper preparation, including salts, sodium monoammonium phosphate, and potassium citrates, to accelerate or control the burning rate. The burn rate has an important effect on the number of puffs that can be obtained by the smoker and the smoke yield. Additionally, filters may contain charcoal, which can adsorb some chemicals and improve taste. Some filters also incorporate additives such as flavorings or methanol. In Fig. 3a) there is the largest mass loss of the sample at ~ 56.53%, which represents the main decomposition stage. This stage is characterized by a DTG peak located at a temperature of 346 °C, which is attributed to the thermal decomposition (pyrolysis) of cellulose acetate, as already mentioned. In the third stage, the sample mass loss is ~ 12.5%, with a residual mass of ~ 6.2% at 600 °C. The thermal results indicate that the r-CA material is more like p-CA than u-CA, and the recovery treatment permits the removal of plasticizers. In Fig. 3b), we have studied and compared the thermal behavior of r-CA 10% PEG and r-CA 15% TAC.

For 10% r-CA PEG, weight loss takes place in a single step, mainly due to breakage of the PEG chains; the largest mass loss of the sample at ~ 85.26% represents the main decomposition stage in a temperature range of 228 to 420 °C. This stage is characterized by a DTG peak located at a temperature of 346 °C, which is attributed to thermal decomposition (pyrolysis) of cellulose acetate (Fig. 3 b)). The materials are stable below 200 °C indicating reasonable thermal stability. The thermal stability of r-CA is high, having an initial degradation temperature above 346 °C.

For r-CA 15% TAC the weight loss takes place in two steps; a significant mass loss of ~ 17.43% manifesting as a DTG peak at 267 °C (Fig. 3b), and this reaction stage is attributed to the thermal decomposition of the plasticizer. Furthermore, there is the largest mass loss of the sample at ~ 63.60%, which represents the main decomposition stage. This stage is characterized by a DTG peak located at a temperature

of 346 °C, which is attributed to the thermal decomposition (pyrolysis) of cellulose acetate as already mentioned. In the third stage the sample mass loss is ~ 12.29%, with a residual mass of ~ 6.2% at 600 °C.

The TMDSC method provides enhancements over conventional DSC in sensitivity and resolution. It enables the differentiation of overlapping events that are challenging or impossible to distinguish using standard DSC, such as simultaneous melting and recrystallization. Modulation facilitates the breakdown of the total heat flow signal into its thermodynamic (heat capacity) and kinetic (irreversible) components. A broad endothermic event between ambient temperature and 100 °C is evident in all the TMDSC sample traces (see Fig. 4a) and b) and is ascribable to the water desorption from the polymer. A second endothermic peak at approximately 230 °C can be visualized for all the traces and is related to the melting of the polymer. The *Tg* of r-CA is 201 °C, for p-CA 196 °C, while for u-CA it is 138 °C. The lower *Tg* of u-CA confirms the presence of plasticizers, because the plasticizers increase the free volume between the polymer chains, spacing them apart. The polymer chains slide through each other at lower temperatures, resulting in a decrease in *Tg*.

The TMDSC of the addition of 10% w/w of PEG (Fig. 5a) and b) leads to a decrease of *Tg* to 160 °C compared to r-CA (*Tg* equal 201 °C), while the addition of 15% TAC leads to a decrease of *Tg* to 112 °C. The *Tg* of the polymer r-CA has been changed by the addition of plasticizers, which has been dramatically reduced with the addition of TAC, so that the hardness has been reduced, the strength has decreased, and the processability has been improved.

A further characterization to evaluate the chemical modification caused by the recovery process and the addition of plasticizer was obtained by ATR-FTIR spectroscopy.

Figure 6a) shows the ATR spectra of the r-CA, u-CA, and p-CA films, while the spectra of the r-CA, r-CA10% PEG, and r-CA 15% TAC films are reported in Fig. 6b). The p-CA film shows a broad peak at 3490 cm-1, which can be attributed to the -OH stretching of non-acetylated cellulose. The absorption band at wave numbers 2942 and 1735 cm^{-1} corresponded to CH stretching of the methyl group (-CH3) and carbonyl stretching of the acetate group (C = O). Other bands at 1642, 1437, 1373, 1211, 1033, and 901 cm^{-1} are H–O-H bending of absorbed water, CH_2 bending, C-H bending vibration of CH_3 of acetyl group, C-O stretching of acetyl group, and C of cellulose backbone and C–O–C stretch, or C–O–C stretch of a glycosidic β-(1 → 4) bond. (Tekin et al. 2023; Cafiero et al. 2023; Fei et al. 2017; De Freitas et al. 2017; Zugenmaier 2004). The ATR spectra of r-CA and u-CA are like those of p-CA, indicating the efficiency of the extraction method proposed in this work. The ATR spectra of the r-CA 10% PEG and r-CA 15% TAC films show no differences with respect to the r-CA spectra. This behavior is because cellulose acetate, TAC, and PEG 400 have the same main functional groups, so the presence of plasticizer in the samples can be detected mainly by increasing the absorbance intensity.

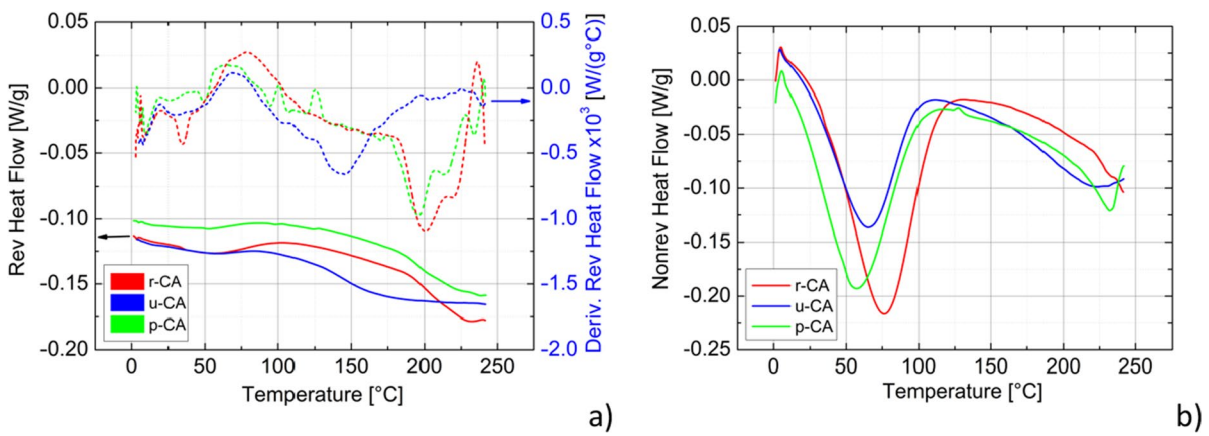

Fig. 4 **a** MDSC Reversing Heat Flow; **b** MDSC Non-Reversing Heat Flow curves of r-CA, u-CA and p- CA films

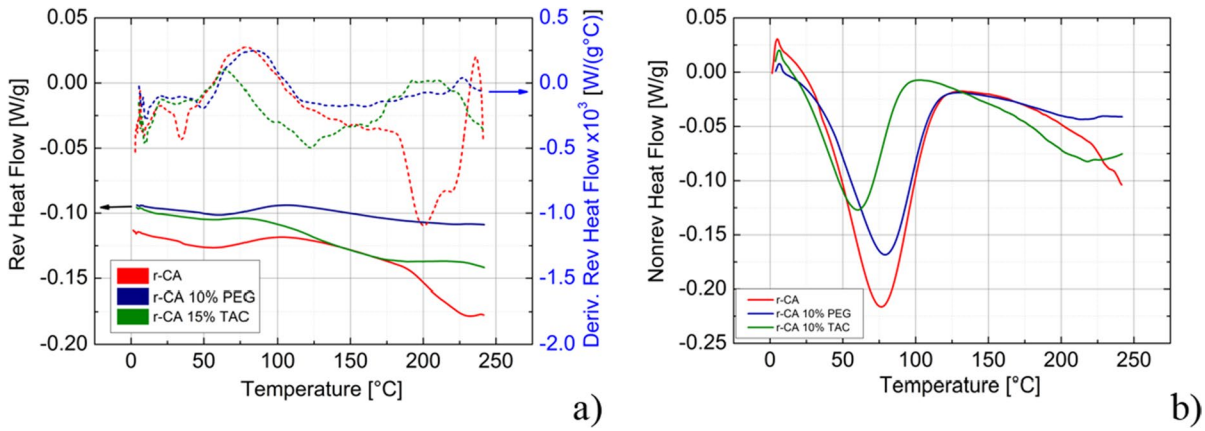

Fig. 5 **a** MDSC Reversing Heat Flow; **b** MDSC Non-Reversing Heat Flow curves of r-CA compared to r-CA 10% PEG, r-CA 15% TAC films

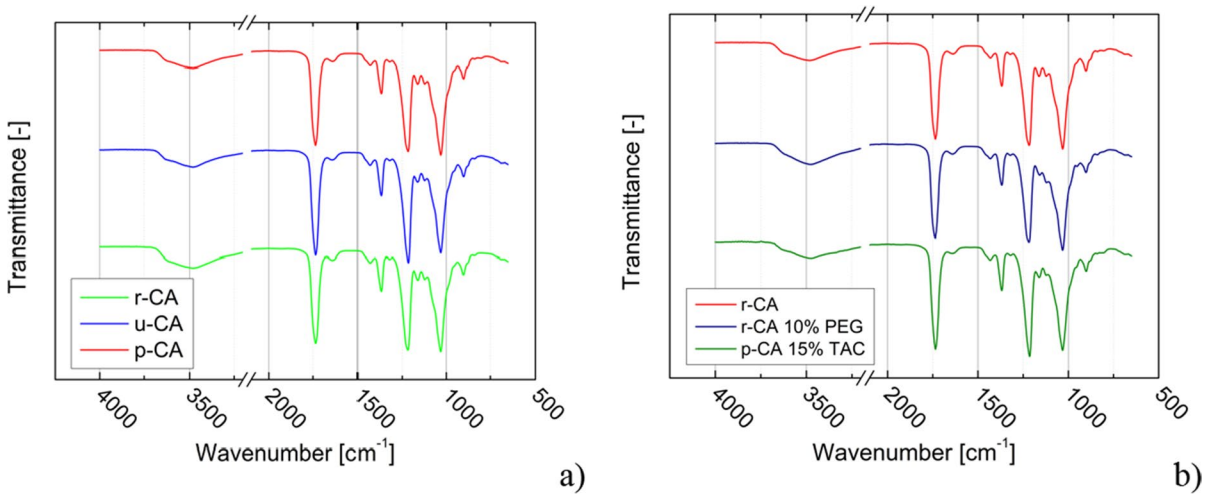

Fig. 6 **a** FT-IR spectra of r-CA, u-CA and p-CA films; **b** FT-IR spectra of r-CA, r-CA 10% PEG and r-CA 15% TAC films

Contact Angle Measurements

The water contact angles of r-CA, p-CA, u-CA, r-CA 10% PEG, and r-CA 15% TAC films are summarized in Table 2.

Samples r-CA, p-Ca, and u-CA show different surface hydrophilicity. Generally, the surface water contact angle of plain CA membrane from commercial polymers is within the range of 50–60°, which can be attributed to variation in surface structure and fabrication parameters and possibly due to the presence of impurities. The unsmoked sample is more hydrophilic than the others because cellulose acetate retains the water-soluble smoke constituents (many of which are irritating, including acids, alkalis, aldehydes, and phenols) while allowing the lipophilic

Table 2 Contact angle results of films r-CA, p-CA, u-CA, r-CA 10% PEG, r-CA 15% TAC

Sample	Contact angle
r-CA	74.7° ± 1.5°
p-CA	65.0° ± 4.0°
u-CA	55.8° ± 1.8°
r-CA 10% PEG 400	46.7° ± 6.8°
r-CA 15% TAC	96.4° ± 2.4°

aromatic compounds. The sample p-CA is a commercial powder of cellulose acetate, not fibers, with a different structural morphology; r-CA is a cellulose acetate fiber recovered after sterilization and extraction, having a different structure fiber. The added PEG increases the hydrophilicity of the cellulose acetate because the value of PEG is hydrophilic and the value is 47°, while the hydrophobicity of TAC increases because the TAC is a hydrophobic polymer.

DMTA results

Cellulose acetate is a brittle material. Plasticization improves the ductility and facilitates melt processing. Therefore, it was of interest to determine whether the PEG and TAC in the formulation could provide the necessary plasticization effect.

To this aim, dynamic mechanical thermal analysis was performed to confirm and gather information on the material structure. The change in glass transition temperature was used to investigate the efficiency of the active compounds as plasticizers for r-CA. This was determined by the peak in the tan δ (*G''/G'*) curves, where *G'* is the elastic modulus and *G''* is the loss modulus. Therefore, Fig. 7a) shows the DMTA thermograms for the recovery of cellulose acetate compared to p-CA and u-CA. The r-CA sample shows a *Tg* of 223 °C, which is consistent with the TMDSC results. Compared to TMDSC, DMTA is more sensitive to changes occurring in *Tg* because the mechanical changes are more dramatic than changes in heat capacity. This is because the DMTA can detect short range motion before the glass transition range is attained and thus identify the onset of main chain motion. p-CA shows a glass transition temperature of 225 °C (a higher value if compared to the TMDSC value, as expected due to the frequency measurement) and a room temperature $G' = 1.23 \times 10^9$ Pa (see Fig. 7a)). Being far below *Tg*, assuming an isotropic linear elastic material with a Poisson's ratio of 0.33, the obtained storage modulus is consistent with the storage modulus in tensile setting usually found in the literature for a similar degree of substitution of 2.5 (Zugenmaier 2004; Guo 1993; Bao et al. 2015). The values of *Tg* and *G'* confirm the TMDSC results, and the recovery material has similar properties and structure to those of p-CA. The u-CA sample shows a *Tg* of 208 °C and $G' = 1.13 \times 10^9$ Pa. The lower value of the glass transition temperature compared to the p-CA and r-CA is caused by plasticizers included in the formulation of commercial cigarette filters.

As shown in Fig. 7b), when plasticizers are added to r-CA, the *Tg* and *G'* decrease. In fact, r-CA with 10% w/w of PEG shows a *Tg* of 133 °C and room temperature $G' = 7.39 \times 10^7$ Pa. *Tg* shows a remarkable decrease of approximately 90 °C in relation to the r-CA sample, while the storage modulus at room temperature decreases by more than one order of magnitude. The effect of the PEG 400 on the thermo-mechanical properties of CA is noticeable; also, the storage modulus starts to drop immediately above room temperature, as supported by compliance values found by Guo 1993. For the r-CA 15% TAC film a *Tg* = 193° C and a room temperature

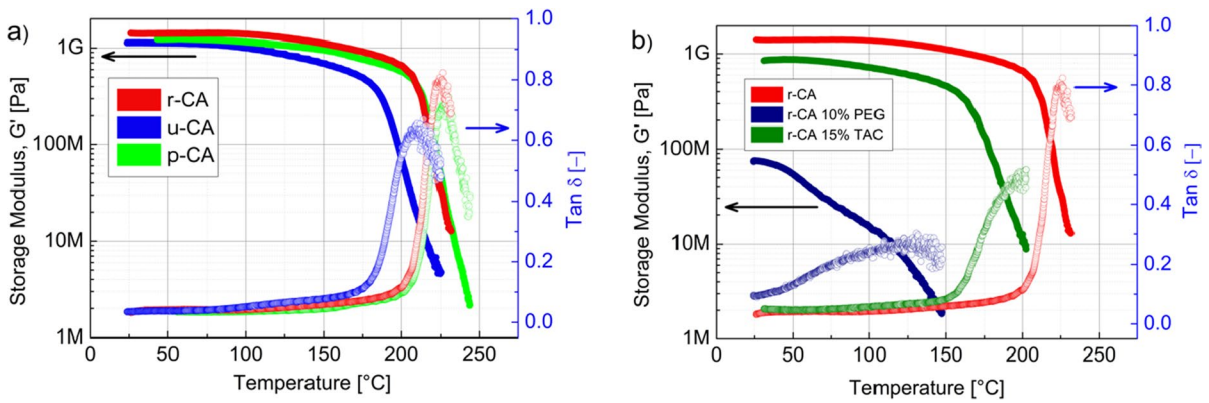

Fig. 7 **a** Storage modulus and damping factor as a function of temperature for r-CA, u-CA, and p-CA films; **b** storage modulus and damping factor as a function of temperature for r-CA, r-CA 10% PEG, and r-CA 15% TAC films

$G' = 8.47 \times 10^8$ Pa are found. The presence of TAC induces a decrease in the storage modulus, consistent with observations from Quintana et al. 2013. Since *Tg* represents a thermodynamic transition, its value for the same material depends on several factors, such as measurement technique, sample geometry, and anisotropy (Idrees et al. 2018).

Rheological studies

Rheological studies are conducted to establish the processability of 3D-printing inks and predict the quality of the printed objects based on factors such as viscoelasticity and viscosity of the inks. Ideally, in 3D printing, inks should exhibit a flow point and shear-thinning behavior to enable a continuous flow of ink through the printing nozzle and rapid recovery of viscosity necessary to maintain the printed object's shape stability (Ebers and Laborie 2020).

The shear thinning behavior of various prepared inks was evaluated by monitoring the change in complex viscosity |η*| with increasing oscillation frequency (Fig. 8). Figure 8a) and 8b) illustrate how the viscosity curve is affected by the solvent content and type, while Figs. 10c) and 10d) compare the rheological behaviour between two samples of cellulose acetate (r-CA and p-CA) under specific solvent conditions (see Table 1). All samples demonstrate a pronounced shear-thinning behaviour typical of pseudoplastic fluids, which exhibit low viscosity at high frequency, and vice versa.

It should be noted that previous research, such as that of Zepnik et al. 2013, has already explored the shear thinning behavior of cellulose acetate mixed

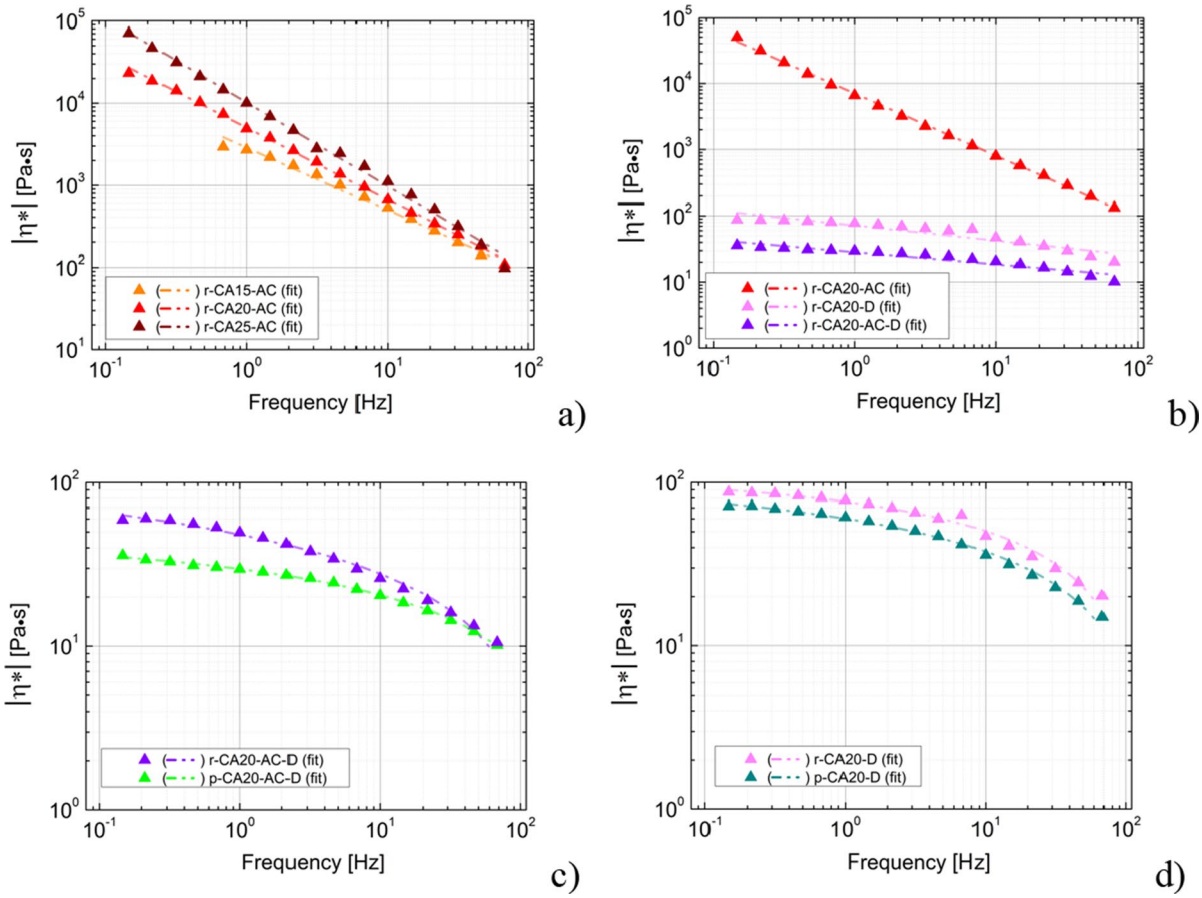

Fig. 8 Complex viscosity at room temperature: **a** effect of acetone content for r-CA based solutions; **b** effect of type of solvent for r-CA based solutions; **c** and **d** comparison between r-CA and p-CA based solutions. Trend lines have been added for each viscosity curve

with a plasticizer, triethyl citrate (TEC), in the melt state at high temperatures. Their results showed that the viscosity remained relatively high for 3D printing, making it less practical for the application. The approach of using solvent-assisted printing at room temperature may be more advantageous, as indicated by the substantial reduction in viscosity when acetone is used as a solvent. Since acetone evaporates rapidly at room temperature, leading to a rapid solidification of the solution during rheological testing, resulting in higher viscosity values, we also considered the dimethyl sulfoxide (DMSO) as a co-solvent or alternative to acetone. In this case the solutions exhibit a different rheological behaviour, combining a Newtonian region at low frequency and a shear-thinning region at high frequency. To quantitatively assess the degree of shear-thinning of these solutions, we fitted their viscosity curves using the Ostwald – de Waele (or power law) viscosity model, which is given by Eq. (1):

$$\eta = k\gamma^{n-1} \tag{1}$$

where η represents viscosity, γ is the shear rate, k is the consistency index, and n is the power law index that defines the viscosity behaviour, i.e., shear thinning ($n<1$), Newtonian ($n=1$), or shear thickening ($n>1$). The equation fitting parameters of the different viscosity curves are summarized in Table 3 and are indicative of the material printability. The consistency index (k) is higher for r-CA in the presence of only AC solvent and increases from 2863 (15 wt % AC) to 8018 (25% wt % AC) with increasing AC content. n for every ink is <1 indicating shear thinning behaviour. Furthermore, n is lower for r-CA in presence of only AC solvent and decreases from 0.23 (15 wt % AC) to 0.12 (25 wt % AC) with increasing AC content, which manifests as shear-thinning behaviour that improves with increasing AC content to improve flowability and better printing performance (Ferrarezi et al. 2013; Liu et al. 2022). The higher k and lower n have also been evaluated for the p-CA-20-AC ink. In Fig. 11 the storage modulus (G') and the loss modulus (G'') as a function of the oscillation frequency are reported for the r-CA-20-AC and r-CA-25-AC inks. As shown in Fig. 9a), the r-CA-20-AC ink shows elastic behaviour or solid-like behaviour ($G''<G'$) in all oscillation frequencies range due to its more complex hydrogen-bonding network and does not exhibit crossover strain (flow point) that guarantees flow during printing due to the transition from solid-like to liquid-like behaviour (Appaw et al. 2007). Instead, a flow point (Fig. 9b) is observed for the CA ink that contains 25% wt of AC, suggesting that its extrusion will produce a stable and accurate 3D printed object. A flow point has also been observed for all inks in which DMSO is present, as observed in Fig. 10.

Table 3 Fitting parameters of the power law for the different solutions

Sample	k (Pa*s^n)	n
r-CA-15-AC	2863	0.23
r-CA-20-AC	7734	0.14
r-CA-25-AC	8018	0.12
r-CA-20-AC-D	20	0.98
p-CA-20-AC-D	23	0.98
r-CA-20-D	33	0.98
p-CA-20-D	32	0.98
p-CA-20-AC	1840	0.24

To check the possibility of using our recovered material as feedstock for SSE 3D printing, we simulated an extrusion process at room temperature by spinning the recovered cellulose acetate mixed with 20% w/w acetone using a syringe. The wire obtained dries quickly in the air, maintaining good homogeneity. In Fig. 11 we show a scheme modification of the syringe for r-CA ink.

The r-CA is stored in a syringe-like reservoir connected to a dispensing nozzle on the printer head. The displacement of the syringe piston and the flow of ink through the nozzle result in stress within the nozzle on the printer head, causing the viscosity of the paste to decrease and the ink to flow (see Fig. 11). As the r-CA is deposited and the stress disappears, the paste relaxes and forms a solid gel, resulting in the successful buildup of 3D objects. Through careful control of ink composition, rheological behavior, and printing parameters, 3D structures that consist of continuous solids, high aspect ratio (e.g., parallel walls), or spanning features can be constructed.

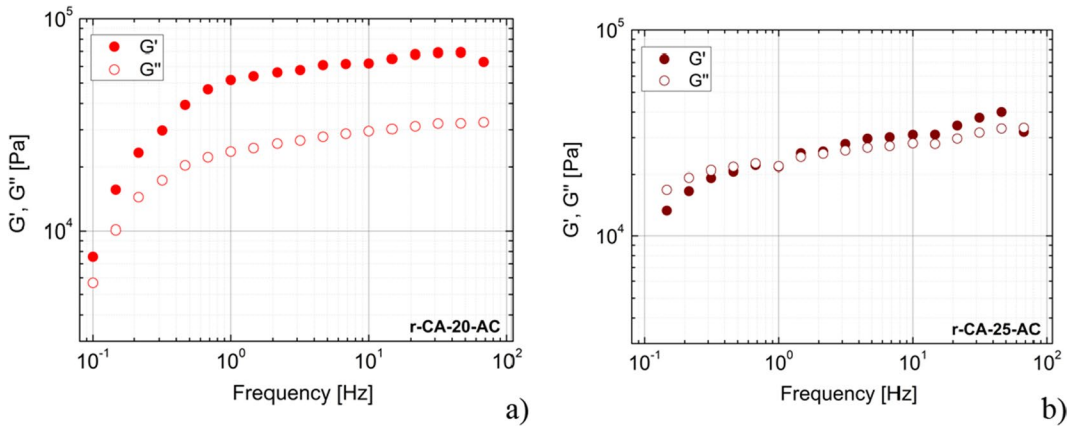

Fig. 9 Storage (*G'*) and loss (*G''*) moduli as functions of frequency for **a**) r-CA15-AC; **b** r-CA20-AC and **c**) r-CA25-AC

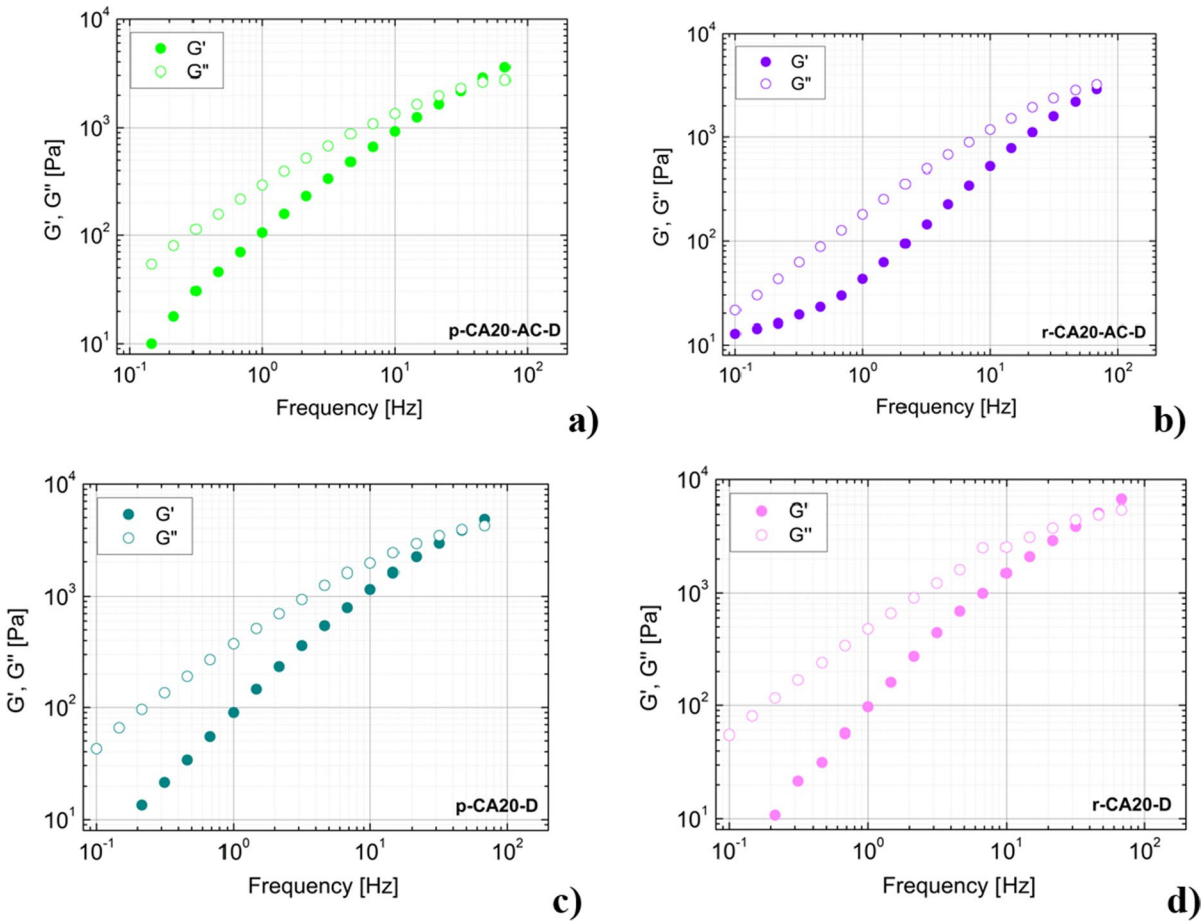

Fig. 10 Storage (*G'*) and loss (*G''*) moduli as functions of frequency for **a**) p-CA20-AC-D; **b** r-CA20-AC-D; **c** p-CA20-D and **d** r-CA20-D

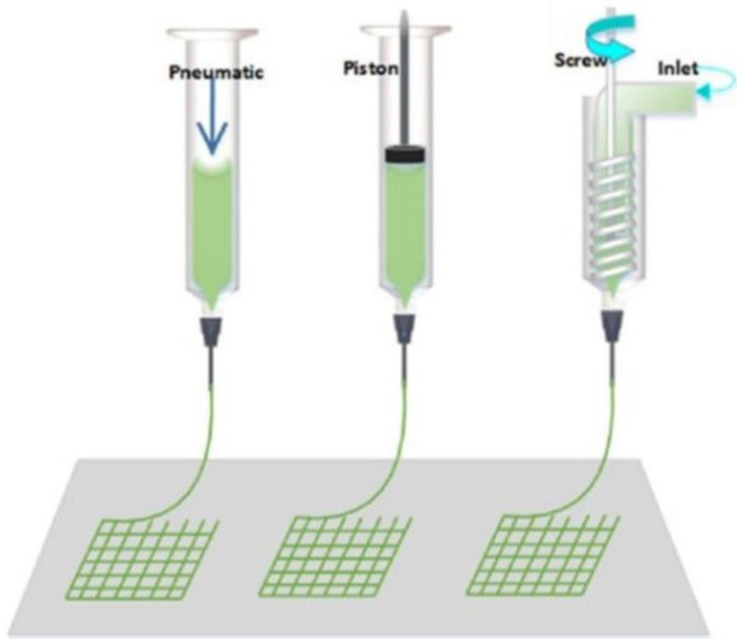

Fig. 11 Scheme of a syringe-like reservoir for r-CA for 3D printing

Conclusions

Cigarette waste poses a significant environmental pollution issue, but it can be recycled by transforming it into raw material to produce new products. Cigarette butts contain various compounds, including aromatic and heterocyclic amines, carbonylated compounds, phenols, polycyclic aromatic hydrocarbons, carbon and nitrogen oxides, and ammonia, which have different solubilities based on their polarity. Leveraging the solubility characteristics, and the main component being cellulose acetate, which dissolves in acetone or ethyl acetate, we propose a method to purify this polymer through sterilization, and we have introduced a dissolution and reprecipitation process resulting in a fine powder, enhancing sample homogeneity and manipulation ease. Characterization using Fourier-transform infrared spectroscopy, thermogravimetric analysis revealed that the purified cellulose acetate maintains structural and thermal properties like those of pure cellulose acetate, while it is very different from untreated cigarette filters, indicating that the purification process does not alter its material properties. The dynamical properties of unplasticized and plasticized cellulose acetate have been investigated by modulated differential scanning calorimetry and dynamic mechanical thermal analysis. The plasticizing effect of PEG and TAC on cellulose acetate was quantified by a decrease in the glass transition temperature as a function of plasticizer content. Rheological studies have been conducted to establish the processability of 3D printing inks and predict the quality of the printed objects based on factors such as the viscoelasticity and viscosity of the inks. It is an eco-friendly option because of the recovery of cellulose acetate from cigarette butts, making it suitable for various applications. However, it is important to note that cellulose acetate can be more difficult to print compared to other thermoplastics and requires careful control of the temperature and printing parameters to achieve optimal results.

Acknowledgments The Authors thank Essequadro eyewear for providing cigarette butts, funding for the ‘green’ extraction study and testing support for the material development.

Authors’ contributions Conceptualization, Lucia Sansone and Flavia D’Urso; methodology, Lucia Sansone and Flavia D’Urso; validation, Michele Giordano; investigation, Lucia Sansone, Flavia D’Urso, Paolo Iaccarino, Maria Oliviero; data curation, Lucia Sansone, Flavia D’Urso, Paolo Iaccarino, Maria Oliviero, Ernesto Di Maio; writing-original draft preparation, Lucia Sansone, Ernesto Di Maio, Paolo Iaccarino.

Funding Open access funding provided by Consiglio Nazionale Delle Ricerche (CNR) within the CRUI-CARE Agreement.

Declarations

Ethical approval Not applicable.

Competing interest The authors declare that they have no known competing financial interests or personal relationships that could have appeared to influence the work reported in this paper.

References

Abdullatif KG, Guirguis MN, Moussa RR (2020) Analysing the structural properties of fire clay bricks after adding cigarette filters. WSEAS Trans Environ Dev 16:671–679. https://doi.org/10.37394/232015.2020.16.69

Appaw C, Gilbert RD, Khan SA, Kadla JF (2007) Viscoelastic behavior of cellulose acetate in a mixed solvent system. Biomacromol 8:1541–1547

Araújo MCB, Costa MF (2019) A critical review of the issue of cigarette butt pollution in coastal environments. Environ Res 172:137–149

Auriemma G, Tommasino C, Falcone G, Esposito T, Sardo C, Aquino RP (2022) Additive manufacturing strategies for personalized drug delivery systems and medical devices: fused filament fabrication and semi solid extrusion. Molecules 27:2784–2847. https://doi.org/10.3390/molecules27092784

Bao CY, Long DR, Vergelati C (2015) Miscibility and dynamical properties of cellulose acetate /plasticizer systems. Carbohydr Polym 116:95–102

Belzagui F, Buscio V, Gutiérrez-Bouzán C, Vilaseca M (2021) Cigarette butts as a microfiber source with a microplastic level of concern. Sci Total Environ 762:144165

Bonanomi G, Maisto G, De Marco A, Cesarano G, Zotti M, Mazzei P, Libralato G, Staropoli A, Siciliano A, De Filippis F, La Storia A, Piccolo A, Vinale F, Crasto A, Guida M, Ercolini D, Incerti G (2020) The fate of cigarette butts in different environments: decay rate, chemical changes and ecotoxicity revealed by a 5-years decomposition experiment. Environ Pollut 261:114108

Browne CL (1990) The Design of Cigarettes. Hoechst Celanese Charlotte, N.C. 119 (BOOK)

Cafiero L, Sorrentino A, Oliviero M (2023) Development of thermo-plasticized cellulose acetate blends for sustainable additive manufacturing. SSRN 4469706. https://ssrn.com/abstract=4469706

Chimene D, Lennox KK, Kaunas RR, Gaharwar AK (2016) Advanced bioinks for 3d printing: a materials science perspective. Ann Biomed Eng 44(6):2090–2102. https://doi.org/10.1007/s10439-016-1638-y

Conradi M, Sanchez-Moyano JE (2022) Toward a sustainable circular economy for cigarette butts, the most common waste worldwide on the coast. Sci Tot Env 847:157634

De Fenzo A, Giordano M, Sansone L (2020) A clean process for obtaining high-quality cellulose acetate from cigarette butts. Materials 13(21):4710

De Freitas RRM, Senna AM, Botaro VR (2017) Influence of degree of substitution on thermal dynamic mechanical and physicochemical. Ind Crops Prod 109:452–458

De Vielmo ASL, Rodrigues AB, da Rosa EV, Domingos DG, Schallemberger JB, Hassemer MEN (2022) Nonwoven from cigarette butt applied in pre-treatment of surface water. Anu Inst Geociênc 45:44159. https://doi.org/10.11137/1982-3908_2022_45_44159

Dieng H, Rajasaygar S, Ahmad AH, Ahmad H, Salmah MdRC, Zuhara WF, Satho T, Miake F, Fukumitsu Y, Saad AR, Ghani IA, Morales Vargas RE, Hafiz A, Majid A, AbuBakar S (2013) Turning cigarette butt waste into an alternative control tool against an insecticide-resistant mosquito vector. Acta Trop 128:584–590

Dieng H, Rajasaygar S, Ahmad AH, Ahmad H, Salmah MdRC, Zuhara WF, Satho T, Miake F, Fukumitsu Y, Saad AR, Ghani IA, Morales Vargas RE, Hafiz A, Majid A, AbuBakar S (2014) Indirect effects of cigarette butt waste on the dengue vector Aedes aegypti (Diptera: Culicidae). Acta Trop 130:123–130

Dobaradaran S, Nabipour I, Saeedi R, Ostovar A, Khorsand M, Khajeahmadi N, Hayati R, Keshtkar M (2017) Association of metals (Cd, Fe, As, Ni, Cu, Zn and Mn) with cigarette butts in northern part of the Persian Gulf. Tob Control 26:461–463

Dobaradaran S, Schmidt TC, Parodi NL, Cegla WK, Jochmann MA, Nabipour I, Lutze HV, Telgheder U (2020) Polycyclic aromatic hydrocarbons (PAHs) leachates from cigarette butts into water. Environ Pollut 259:113916

Dreux X, Majesté JC, Carrot C, Argoud A, Vergelati C (2019) Viscoelastic behavior of cellulose acetate/triacetin blends by rheology in the melt state. Carbohydr Polym 222:114973

Ebers LS, Laborie MP (2020) Direct ink writing of fully bio based liquid crystalline lignin/hydroxypropyl cellulose aqueous inks: optimization of formulations and printing parameters. ACS Appl Bio Mater 3:6897–6907

Fei P, Liao L, Cheng B, Song J (2017) Quantitative analysis of cellulose acetate with a high degree of substitution by FTIR and its application. Anal Methods 9:6194–6201

Ferrarezi MMF, Rodrigues GV, Felisberti MI, Goncalves MdC (2013) Investigation of cellulose acetate viscoelastic properties in different solvents and microstructure. Eur Polym J 49:2730–2737

Finster P, Hollweg J, Seehofer F (1986) Determination of triacetin in cigarette filters by pulsed nuclear magnetic resonance spectroscopy-Bestimmung von triacetin in zigarettenfiltern mit hilfe der gepulsten kernresonanzspektroskopie. Beiträge Zur Tabak Int 13:255–264

Gatenholm P, Martinez H, Karabulut E, Amoroso M, Ko¨lby L, Markstedt K, Gatenholm E, Henriksson I (2016) Development of nanocellulose-based bioinks for 3d bioprinting of soft tissue. In: Ovsianikov A, Yoo J, Mironov V (eds) 3d printing and biofabrication. Springer Cham 1–23. https://doi.org/10.1007/978-3-319-40498-1_14-1

Ghasemi A, Mofrad MMG, Parseh I, Hassani G, Mohammadi H, Hayati R, Alinejad N (2022) Cigarette butts as a super challenge in solid waste management: a review of current knowledge. Environ Sci Pollut Res 29:51269–51280

Gibson I, Rosen D, Stucker B (2015) Additive manufacturing technologies: 3D printing, rapid prototyping, and direct digital manufacturing. Springer-Verlag, New York, 498. https://doi.org/10.1007/978-1-4939-2113-3

Gómez Escobar V, Moreno González C, Arévalo Caballero MJ, Gata Jaramillo AM (2021) Initial conditioning of used cigarette filters for their recycling as acoustical absorber materials. Materilas 14:416. https://doi.org/10.3390/MA14154161

Green ALR, Putschew A, Nehls T (2019) Littered cigarette butts as a source of nicotine in urban waters. J Hydrol 519:3466–3474

Guo JH (1993) Effects of plasticizers on water permeation and mechanical properties of cellulose acetate antiplasticization in slightly plasticized polymer film. Drug Dev Ind Pharm 19:1541–1555

Idrees M, Jeelani S, Rangari V (2018) Three-dimensional-printed sustainable biochar-recycled PET composites. ACS Sustain Chem Eng 6:13940–13948

Islam MR, Khan ANN, Mahmud RU, Haque SMN, Khan MMI (2022) Sustainable dyeing of jute-cotton union fabrics with onion skin (allium CEPA) dye using banana peel (Musa) and guava leaves (Psidium guajava) extract as biomordants. Pigm Resin Technol 53(4):1–7. https://doi.org/10.1108/prt-03-2022-0031

Jungst T, Smolan W, Schacht K, Scheibel T, Groll J (2016) Strategies and molecular design criteria for 3d printable hydrogels. Chem Rev 116(3):1496–1539. https://doi.org/10.1021/acs.chemrev.5b00303

Kalsoom U, Nesterenko PN, Paull B (2016) Recent developments in 3d printable composite materials. RSC Adv 6(65):60355–60371. https://doi.org/10.1039/c6ra11334f

Kataržytė M, Balčiūnas A, Haseler M, Sabaliauskaitė V, Lauciūtė L, Stepanova K, Nazzari C, Schernewski G (2020) Cigarette butts on Baltic Sea beaches: Monitoring, pollution, and mitigation measures. Mar Pollut Bull 156:111248

Kirchmajer DM, Gorkin R, Panhuis M (2015) An overview of the suitability of hydrogel-forming polymers for extrusion-based 3d-printing. J Mater Chem B 3(20):4105–4117. https://doi.org/10.1039/c5tb00393h

Kurmus H, Mohajerani A (2020) The toxicity and valorisation options of cigarette butts. Waste Manag 104:104–118

Lee M, Kim GP, Don Song H, Park S, Yi J (2014) Preparation of energy storage material derived from a used cigarette filter for a supercapacitor electrode. Nanotechnol 25. https://doi.org/10.1088/0957-4484/25/34/345601

Lee W, Lee CC (2015) Developmental toxicity of cigarette butts. An underdeveloped issue ecotoxicol. Environ Saf 113:362–368

Li T, Aspler J, Kingsland A, Cormier LM, Zou X (2016) 3d printing a review of technologies, markets, and opportunities for the forest industry. J-for 5(2):30–37

Ligon SC, Liska R, Stampfl J, Gurr M, Mulhaupt R (2017a) Polymers for 3d printing and customized additive manufacturing. Chem Rev 117(15):10212–10290. https://doi.org/10.1021/acs.chemrev.7b00074

Ligon SC, Liska R, Stampfl J, Gurr M, Mülhaupt R (2017) Polymers for 3D printing and customized additive manufacturing. Chem Rev 117:10212

Liu L, Gong D, Bratasz L, Zhu Z, Wang C (2019) Degradation markers and plasticizer loss of cellulose acetate films during ageing. Polym Degrad Stab 168:108952

Liu G, Bhat MP, Kim CS, Kim J, Lee KH (2022) Improved 3D-printability of cellulose acetate to mimic water. Macromolecules 55:1855–1865

Mahmud RU, Momin A, Islam R, Siddique AB, Khan AN (2022) Investigation of mechanical properties of pineapple-viscose blended fabric reinforced composite. Compos Adv Mater 31:1–10. https://doi.org/10.1177/26349833221087752

Micevska T, Warne MSJ, Pablo F, Patra R (2006) Variation in, and causes of, toxicity of cigarette butts to a cladoceran and microtox. Bull Environ Contam Toxicol 50:205–212

Mohajerani A, Kadir AA, Larobina L (2016) A practical proposal for solving the world's cigarette butt problem: recycling in fired clay bricks. J Waste Manag 52:228–244

Mohajerani A, Bakaric J, Jeffrey-Bailey T (2017) The urban heat island effect, its causes, and mitigation, with reference to the thermal properties of asphalt concrete. Environ Manag 197:522–538

Novotny TE, Hardin SN, Hovda LR, Novotny DJ, McLean MK, Khan S (2011) Tobacco and cigarette butt consumption in humans and animals. Tob Control 20:i17–i20

Oskui SM, Diamante G, Liao C, Shi W, Gan J, Schlenk D, Grover WH (2015) Assessing and reducing the toxicity of 3d-printed parts. Environ Sci Technol Lett 3(1):1–6. https://doi.org/10.1021/acs.estlett.5b00249

Parker TT, Rayburn J (2017) A comparison of electronic and traditional cigarette butt leachate on the development of Xenopus laevis embryos. Toxicol Rep 4:77–82

Piras CC, Fernandez-Prieto S, De Borggraeve WM (2017) Nanocellulosic materials as bioinks for 3d bioprinting. Biomater Sci 5(10):1988–1992. https://doi.org/10.1039/c7bm00510e

Quintana R, Persenaire O, Lemmouchi Y, Sampson J, Martin S, Bonnaud L, Dubois P (2013) Enhancement of cellulose acetate degradation under accelerated weathering by plasticization with eco-friendly plasticizers. Polym Degrad Stab 98:1556–1562

Rahman MT, Mohajerani A, Giustozzi F (2020) Possible use of cigarette butt fiber modified bitumen in stone mastic asphalt. Constr Build Mater 263:120134. https://doi.org/10.1016/j.conbuildmat.2020.120134

Rejeski D, Zhao F, Huang Y (2018) Research needs and recommendations on environmental implications of additive

manufacturing. Addit Manuf 19:21–28. https://doi.org/10.1016/j.addma.2017.10.019
Shen X, Shamshina JL, Berton P, Gurau G, Rogers RD (2016) Hydrogels based on cellulose and chitin: fabrication, properties, and applications. Green Chem 18(1):53–75. https://doi.org/10.1039/c5gc02396c
Slaughter E, Gersberg RM, Watanabe K, Rudolph J, Stransky C, Novotny TM (2019) Toxicity of cigarette butts, and their chemical components, to marine and freshwater fish. Tob Control 20:i25–i30
Sultan S, Siqueira G, Zimmermann T, Mathew AP (2017) 3d printing of nano-cellulosic biomaterials for medical applications. Curr Opin Biomed Eng 2(Supplement C):29–34. https://doi.org/10.1016/j.cobme.2017.06.002
Tekin FS, Çulfaz-Emecen PZ (2023) Controlling cellulose membrane performance via solvent choice during precursor membrane formation. ACS Appl Polym Mater 5(3):2185–2194. https://doi.org/10.1021/acsapm.2c02185
Torkashvand J, Farzadkia M, Sobhi HR, Esrafli A (2020) Littered cigarette butt as a well-known hazardous waste: a comprehensive systematic review. J Hazard Mater 383:121242
Torkashvand J, Godini K, Norouzi S, Gholami M, Yeganeh M, Farzadkia M (2021) Effect of cigarette butt on concentration of heavy metals in landfill leachate: health and ecological risk assessment. J Environ Health Sci Eng 19:483–490
Torkashvand J, Saeedi-Jurkuyeh A, Kalantary RR, Gholami M, Esrafili A, Yousefi M, Farzadkia M (2022) Preparation of a cellulose acetate membrane using cigarette butt recycling and investigation of its efficiency in removing heavy metals from aqueous solution. Sci Rep 12:20336
Valiente R, Escobar F, Pearce J, Bilal U, Franco M, Sureda X (2020) Estimating and mapping cigarette butt littering in urban environments: a GIS approach. Environ Res 183:109142
Wang X, Jiang M, Zhou Z, Gou J, Hui D (2017) 3d printing of polymer matrix composites: a review and prospective. Compos B Eng 110:442–458. https://doi.org/10.1016/j.compositesb.2016.11.034
Yousef M, Kermani M, Farzadkia M, Godini K, Torkashvand J (2021a) Challenges on the recycling of cigarette butts. Environ Sci Pollut Res 28:30452–30458
Yousef M, Oskoei V, Jafari AJ, Farzadkia M, Firooz MH, Abdollahinejad B, Javavd T (2021b) Municipal solid waste management during COVID-19 pandemic: effects and repercussions. Environ Sci Pollut Res 28:32200–32209
Yousef S, Eimontas J, Striugas N, Praspaliauskas M, Abdelnaby MA (2022) Pyrolysis kinetic behavior; TG-FTIR, and GC/MS analysis of cigarette butts and their components. Biomass Conv Bioref. https://biblioproxy.cnr.it:2481/10.1007/s13399-022-02698-5
Zepnik S, Kabasci S, Kopitzky R, Radusch HJ, Wodke T (2013) Extensional flow properties of externally plasticized cellulose acetate: influence of plasticizer content. Polymers 5:873–889
Zugenmaier P (2004) Characterization and physical properties of cellulose acetates. Macromol Symp 208(81):166